USING LAND COVER DATA TO IMPROVE ESTIMATED SNOWPACK PROPERTIES BY MICROWAVE DATA

Amir E Azar*, Tarendra Lakhankar, Hosni Ghedira, Peter Romanov, Narges Shahroudi Reza Khanbilvardi,
NOAA-CREST, City University of New York, New York, NY

Abstract- Snow pack properties such as snow depth and snow water equivalent (SWE) have always attracted hydro-meteorologists. The satellite borne microwave imagery has provided the option to produce spatial SWE distribution maps. This research focuses on application of passive microwave data to estimate SWE developing an algorithm to estimate snowpack properties in Great Lakes area based on a three-year of SSM/I dataset along with corresponding ground truth data. The study area is located between latitudes 41N-49N and longitudes 87W-98W. The area is covered by 28*35 SSM/I EASE-Grid pixels with spatial resolution of 25km. Nineteen test sites were selected based on seasonal average snow depth, and land cover type. Each of the sites covers an area of 25km*25km with minimum of one snow reporting station inside. Two types of ground truth data were used: 1) point-based snow depth observations from NCDC; 2) grid based SNODAS-SWE dataset, produced by NOHRSC. To account for land cover variation in a quantitative way NDVI data were used. To do the analysis, three scattering signatures of GTVN (19V-37V), GTH (19H-37H), and SSI (22V-85V) were derived. The analysis shows that at lower latitudes of the study area there is no correlation between GTH and GTVN versus snow depth. On the other hand SSI shows an average correlation of 75 percent with snow depth in lower latitudes which makes it suitable for shallow snow identification. In the model development a non-linear algorithm was defined to estimate SWE using SSM/I signatures along with the NDVI values of the pixels. The results show up to 60 percent correlation between the estimated SWE and ground truth SWE. The results showed that the new algorithm improved the SWE estimation by more than 20 percent for specific test sites.

* *Corresponding author address:* Amir E. Azar, The City College of New York, Dept. of Civil Engineering, New York, NY, 10031;
e-mail: aeazar@ce.ccny.cuny.edu

Introduction

Understanding seasonal variation of snowcover and snowpack properties is of critical importance for effective management of water resources. Satellites operating in the optical wavelength have monitored snowcover over the Northern Hemisphere for more than thirty years (Grody et al. 1996). Optical sensors can detect snowcover during daylight and under cloud-free conditions. In contrast to visible bands, remote measurements operation in microwave region offers the potential of monitoring the SWE and snow wetness due to penetrating capability of absorption of the emitted radiation at microwave frequencies. Hallikainen et al. (1984) introduced an algorithm for estimating SWE using passive microwave Scanning Multi-channel Microwave Radiometer (SMMR) data. The process involved the subtraction of a fall image from a winter image in the vertical polarization of 18 and 37 GHz frequencies. The difference, ΔT, was used to define linear relationships between ΔT and SWE.

Chang et al. (1987) related the difference between the SMMR brightness temperatures in 37 GHz and 18 GHz channels to derive snow depth – brightness temperature relationship for a uniform snow field SD=1.59(Tbh19-Tbh37). This equation assumes a constant density and grain size for the snowpack. Goodison and Walker (1995) introduced another algorithm to estimate SWE using SSM/I channels. They used vertical gradient (GTV) between brightness temperatures at 37GHz and 19 GHz and defined a linear relationship

between SWE and GTV. This gradient value is obtained by subtracting the brightness temperature, Tb at frequencies of 37 and 19 GHz and dividing it by a constant (Goodison, Walker 1995). Goodson-Walker algorithm has been used widely in North America over Great Plains and Canada. Derksen (2004) carried out a detailed evaluation of SWE and SCE derived using SMMR and SSM/I data over the south Central part of Canada. The new technique to infer SWE from satellite data incorporated different algorithms for open environments, deciduous, coniferous, and spars forest cover and calculated SWE as weighted average of all four estimates: $SWE=F_D SWE_D+F_C SWE_C+F_S SWE_S+F_O SWE_O$, where (F) is the fraction of each land cover type within a pixel, D, C, S, and O correspondingly represent deciduous forest, coniferous forest, S sparse forest, and O open prairie environments. Passive microwave dataset and in situ SWE observation were compared and showed that the SMMR brightness temperature adjustments are required to produce SWE that fits SWE inferred from SSM/I.

The above algorithms used the spectral difference between microwave channels from various sensors to estimate SWE or snow depth. However other snow or land parameters such as snow grain size, land cover type, and snow conditions have effects on scattering in microwave. Although, some researchers have introduced land cover type to their models, their algorithms were developed and validated regionally so those can not applied in other study areas. In addition, these algorithms use multi-regression approaches to account for the land cover type. Development of an algorithm which quantitatively considers variation of land cover for different areas is necessitated. The Normalized Difference Vegetation Index (NDVI) has been widely used to represent the health and greenness of the vegetation. In this study a non-linear algorithm is proposed, which estimates SWE using spectral difference between SSM/I channels along with NDVI.

DATA USED

SSM/I Data

The SSM/I passive microwave radiometer has seven channels operating at five frequencies (19, 35, 22, 37.0, and 85.5 GHz) and dual- polarization (except at 22GHz which is vertical polarization only). The sensor spatial resolution varies for different channels frequencies. In this study the Scalable Equal Area Earth Grid EASE-Grid SSM/I products distributed by National Snow and Ice Data Center (NSIDC) were used. EASE-Grid spatial resolution is slightly more than 25km (25.06km) for all the channels (NSIDC) however the spatial resolution of the microwave spectrum at longer wavelengths is more than 50km. This study employed a Northern Hemisphere Azimuthal Equal-Area (EASE-Grid) projection.

Normalized Difference Vegetation Index (NDVI)

Proposed by Rouse et al. (1973), NDVI was originally used to locate vegetation in Great Plains. NDVI is defined as a difference between reflectance in visible and near infrared spectral bands divided by their sum NDVI = (NIR-VIS)/(NIR+VIS). Live green plants appear relatively dark in the visible and relatively bright in the near-infrared (Gates 1980). By contrast, clouds and snow tend to be rather bright in the visible and quite dark in the near-infrared. Then, highly vegetated lands such as forests tend to have higher NDVI while low vegetated areas such as grass lands have low NDVI. Soil and bare land have very low NDVI which even becomes negative if the land is covered by snow.

The NDVI data for this study were obtained from the NOAA/NASA Pathfinder Advanced Very High Resolution Radiometer (AVHRR) dataset which is distributed by Goddard Space Flight Center (GSFC). The NDVI data are extracted from a global 10-day composite image for January 21 to31 in 1994. The composite images are derived from images in a 10-day period with minimum cloud coverage. To facilitate the comparison and matching of the two datasets (NDVI and SSM/I) NDVI data resampled and projected to the same EASE-Grid projection at 25km spatial resolution.

NDVI has a seasonal pattern meaning that it increases during spring and summer and decreases during winter. The winter NDVI tend to be much lower than summer for all types of land cover. Also, NDVI variation during the winter season is very limited. Maximum winter NDVI is generally observed over evergreen needle-leaf forests. Winter NDVI tends to decrease over mixed forests and deciduous broad-leaf forests. Over grass land and bare land which is covered by snow NDVI becomes negative. One of the sources of error in estimating SWE from microwave data is attenuation of microwave scattering over the forested areas (evergreen and mixed forests). By using winter NDVI data, the scattering attenuation effect can be minimized.

Ground Truth Snow Measurements

Point Gauge Measurements

Surface observations of snow were obtained from National Climate Data Center (NCDC). US climate monitoring data center in NCDC provides daily snow depth data from all reposting station throughout US. For selected test sites (each site size of an EASE-Grid pixel, which will be discussed in the next section) the corresponding snow depth measurements were averaged to determine the snow depth.

SNODAS SWE

Snow products generated by the Snow Data Assimilation System (SNODAS) of NOAA National Weather Service's National Operational Hydrologic Remote Sensing Center (NOHRSC), are available beginning October 2003. SNODAS includes a procedure to assimilate airborne gamma radiation and ground-based observations of snow covered area and snow water equivalent, downscaled output from Numerical Weather Prediction (NWP) models combined in a physically based, spatially-distributed energy and mass balance model. The output products have 1km spatial and hourly temporal resolution. In order to match the EASE-Grid pixels the SNODAS SWE data were averaged to 25km.

METHOD

The study area is located in Great Lakes area between latitudes 41^{o} N-49^{o} N and longitudes 87^{o} W-98^{o} W covering parts of Minnesota, Wisconsin and Michigan. The area is covered by 980 (28 by 35) EASE-Grid pixels. For the time series analysis 19 test sites were selected. Each site, 25km x 25km, represents an SSM/I pixel. The sites were selected based on their latitude and their land cover type along with the annual snow accumulation. Low standard deviations for NDVI in each test sites shows the limited variation of land cover type within each test site (Table 1). To avoid wet snow conditions only the period from December 1 of each year to the February 28 of the following year are considered. Three 90-day of data sets were derived for each winter.

Data Analysis

Table 1 lists geographical location of the selected test sites and their NDVI characteristics including the mean value and standard deviation. The mean and standard deviation are derived based on difference between spatial resolution of EASE-Grid, 25km x 25km, NDVI, 8km x 8km.

Each test site is size of an EASE-Grid pixel (25km x 25km) while NOHRSC SNODAS SWE data are in 1km spatial resolution. To derive the SWE over each test site the NOHRSC SWE data was averaged to 25km resolution. Figure 1 illustrates the mean and standard deviation of SWE for different days in test sites 2, 9, and 17.

In this study the correlation between SSM/I channels and snow depth and SWE for different types of land cover located in different latitudes is used. Three years of (2002-2004) SSM/I channels versus snow depth and SWE for each of the selected sites were derived. The SSM/I data were obtained from the descending pass of Defense Meteorological Satellite Program (DMSP) satellites. There are three SSM/I scattering signatures used in this analysis. The first scattering signature, GTH (19H - 37H), is the difference between 19 and 37GHz in horizontal polarization. The second signature, GTVN (19V-37V) shows the difference between vertically polarized 19 and 37GHz. Finally, SSI (22V-85V) is the difference between 22 and 85 GHz in

vertical polarization. SSI can be used to identify shallow snowcover. A graphical representation of correlation coefficients of snow depth versus GTVN, GTH, and SSI for all the test sites is shown in Figure 2.

Table 1: Coordinates of selected pixels along with NDVI values, Each EASE-Grid pixel contains 3 x 3 NDVI Pixels

Test Site	SSM/I EASE-Grid Pixels		NDVI		
	Latitude	Longitude	Center	Mean	Standard Deviation
1	42.33	-93.62	-0.040	-0.033	0.008
2	42.89	-91.97	-0.040	-0.038	0.005
3	43.63	-91.43	-0.032	-0.025	0.012
4	44.14	-90.57	0.136	0.121	0.020
5	44.39	-89.12	0.000	0.032	0.016
6	45.12	-89.11	0.016	0.034	0.018
7	46.07	-88.19	0.272	0.219	0.029
8	45.59	-88.21	0.192	0.237	0.024
9	46.09	-88.79	0.256	0.268	0.024
10	46.80	-88.46	0.304	0.196	0.026
11	46.80	-88.16	0.176	0.234	0.023
12	46.83	-89.69	0.248	0.247	0.026
13	45.36	-91.18	0.032	0.038	0.022
14	45.56	-92.68	-0.024	0.023	0.015
15	47.26	-92.78	0.168	0.123	0.018
16	48.01	-91.88	0.160	0.212	0.025
17	47.92	-94.08	0.056	0.079	0.020
18	48.40	-95.99	0.056	0.035	0.017
19	47.47	-97.47	-0.024	-0.026	0.007

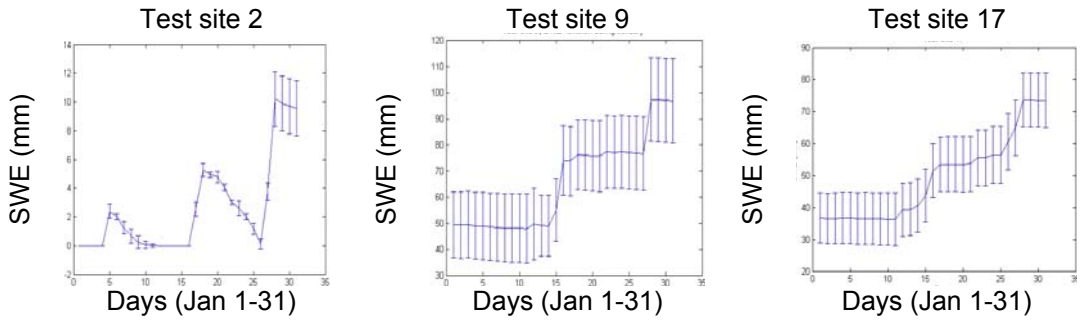

Figure 1. Variation of SWE obtained from NOHRSC (1km x 1km) for Different Test Sites (25kn x 25km), Winter 03-04

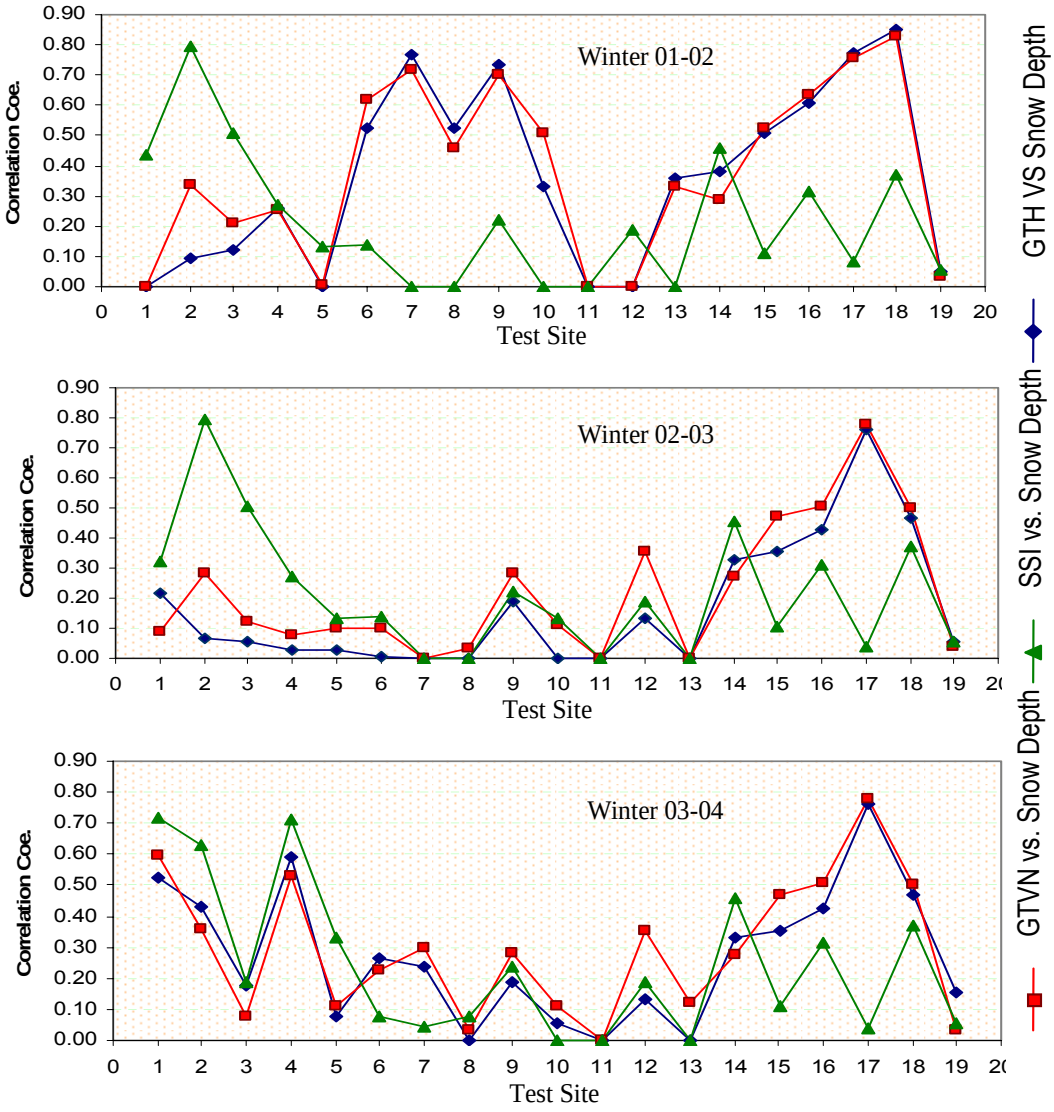

Figure 2. Correlations of snow depth vs. SSM/I signatures GTVN (19v-37v), GTH(19h-37h), and SSI(22v-85v) for various test sites (TS) for winter seasons 01-02, 02-03, 03-04

The scatter plots of SWE versus SSM/I scattering signature are shown in Figure 3. Different slopes of the regression lines indicate attenuation of the scattering due to the land cover variation. The land cover variation can be represented by NDVI value for each of the test sites. For the test sites with higher NDVI, the regression slope is larger and for lower NDVI values the regression slope is smaller (Fig 4).

2.19.6

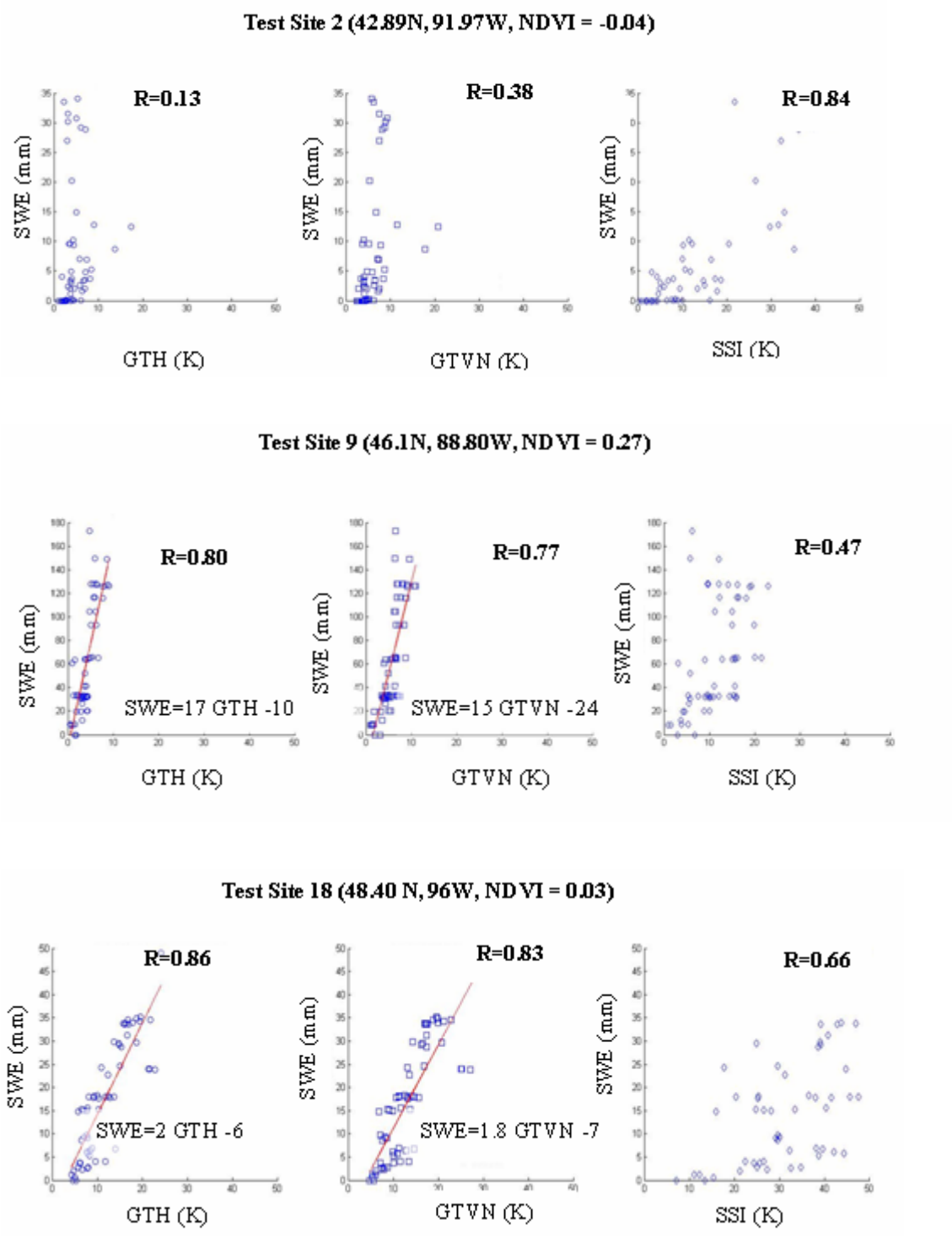

Figure 3. SSM/I scattering signatures signature ((GTH (19H-37H), GTVN (19H-37V), and SSI (22H-85H)) vs. SWE (SNODAS) for winter 2003-2004

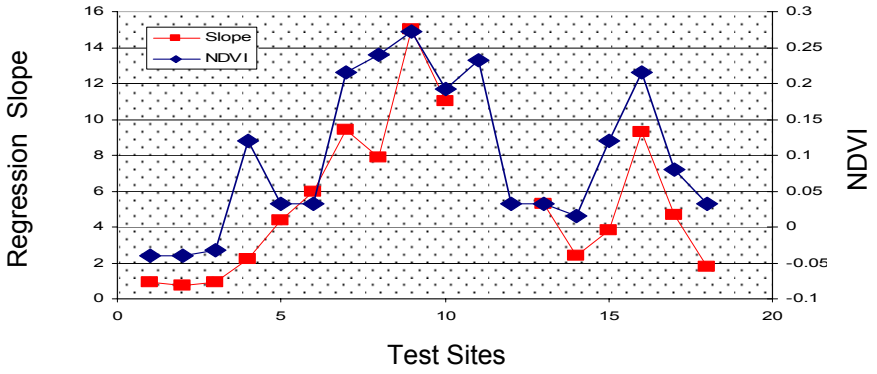

Figure 4. Variations of the slope of the regression lines in the scatter plots with NDVI for the test sites for winter 03-04, SWE vs. GTVN

The scatter plot of the regression slopes versus NDVI is illustrated in Figure 5. It is shown that the regression slope and the NDVI are highly correlated represented by R^2 and the regression line. As mentioned before each of the selected test sites are size of an EASE-Grid pixel (25km x 25km) and the study area consists of 980 pixels from which 19 were selected as test sites. As shown in Figure 5, by having the regression line and the NDVI for each EASE-Grid pixel the regression slope for that particular grid can be derived. In other words, higher NDVI of a grid results in higher factors in SWE estimating equations.

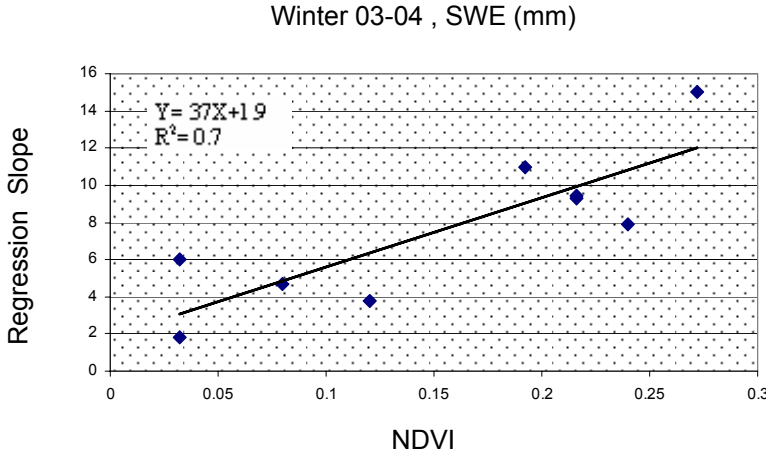

Figure 5. Scatter plots of the regression lines vs. NDVI

Considering the facts mentioned above we propose a new algorithm which relates SWE and the SSM/I scattering signature GTVN (19v-37v) and accounts for possible variation of NDVI:

SWE=F (A* NDVI* + B)*GTVN,*
While NDVI >= 0
*SWE=C*SSI+D*
While NDVI <0

Where SWE is the snow water equivalent in mm, GTVN (19v-37v), and SSI

(22v-85v) are SSM/I spectral scattering signatures. Winter time NDVI was obtained from a 10-day composite image for January 1994. In the formula above F is a coefficient accounting for small variations on NDVI during the winter season. A and B are derived from the scatter plots of regression slope and NDVI. Coefficients C and D are determined from the scatter plots of SWE versus SSI using the average of the best fitted line to the scatter plots. The Values of coefficients A, B, C, and D entering the above formula were found equal to 35, 2, 0.9, and -3 respectively. In the case of little or no vegetation protruding through the snow pack the NDVI value is close to zero and the formula above simplifies to Goodison-Walker algorithm. Figure 6 illustrates the behavior of the new algorithm for transition between NDVI<0 to NDVI>=0.

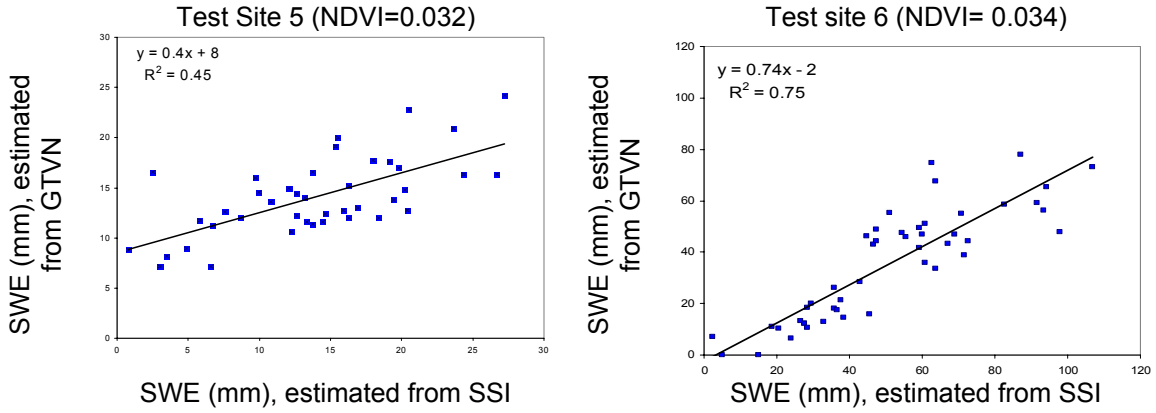

Figure 6. Comparison of SWE estimated by SSI and GTVN

Algorithm Validation

The new algorithm was examined over the whole dataset of matched satellite retrieval and SWE estimates in Great Lakes region. Figure 7 shows the results obtained with the new algorithm over test site 10 as compared to Goodison-walker and Chang algorithms. The tests site 10 is located in latitude 46.8N and longitude -88.46W in the area covered with mixed forest. Besides the temporal validation, the new algorithm was spatially validated for the whole study area (Latitudes: 41N to 49N & Longitudes: -87W to-98W). There were eleven days (3 days December, 4 days January, and 4 days February) in winter 2003-2004 selected. For those days the full coverage of the study area from SSM/I data was available. The ground truth data was obtained by averaging NOHRC SNODAS dataset. Figure 8 shows the ground truth and estimated SWE for January 25, 2004.

The NDVI image of the study area (Fig 9) shows higher values of NDVI around the lake. This is the area that both Chang and Goodison-Walker algorithms highly underestimate the SWE (Fig 10). In contrast, the new non-linear algorithm can estimate SWE in the area in the vicinity of the lake with much higher accuracy (Fig 11). The calculated RMSE and correlation coefficient (R2) are shown for all the three algorithms. The use of NDVI in the new algorithm results in a decrease of the RMSE and the increase of the correlation coefficient. It also increases the range for the estimated SWE. Figure 19 demonstrates a consistent improvement in the accuracy of the estimated SWE for the winter season of 2003-2004.

For all days, application of the new developed algorithm results in the highest correlation coefficient between SSM/I and SWE. At the same time, the RMSE of SWE derived with the new algorithm is lower for all days but one. There is a decreasing trend of in correlations and increasing trend in SWE in February. The most probable reason for this trend is snow melt. In February, the study area and especially its southern part experienced several melt and

refreeze of snow. The higher brightness temperature and reported surface temperatures over the study area supports the existence of wet snow for those days. Estimates of snow depth and SWE with satellite observations in microwave become practically impossible when snow is wet.

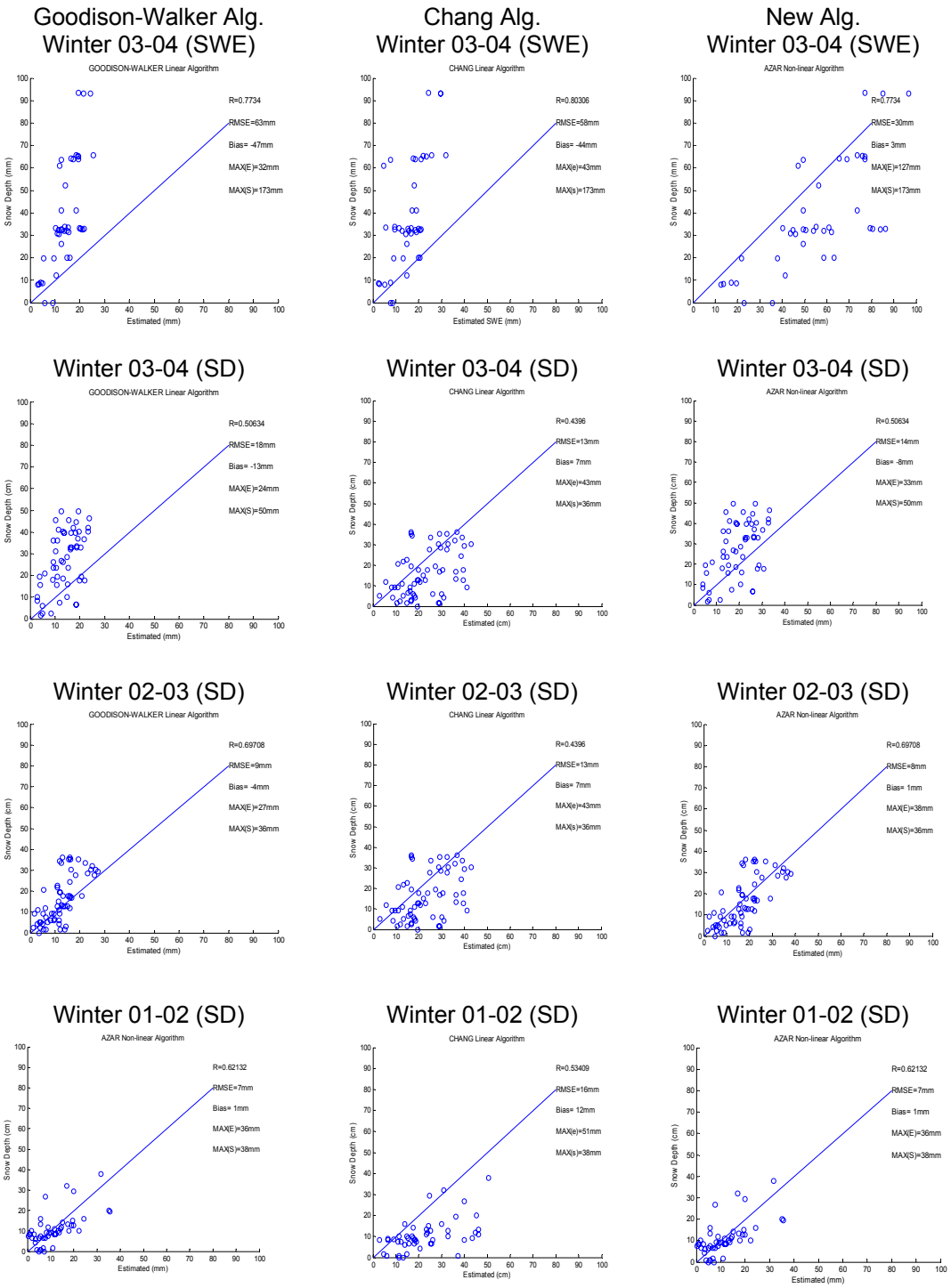

Figure 7. Comparison of the results for different algorithms for test site 10 (Lat = 48.6N, Lon = -88.46W, and NDVI = 0.2)

2.19.10

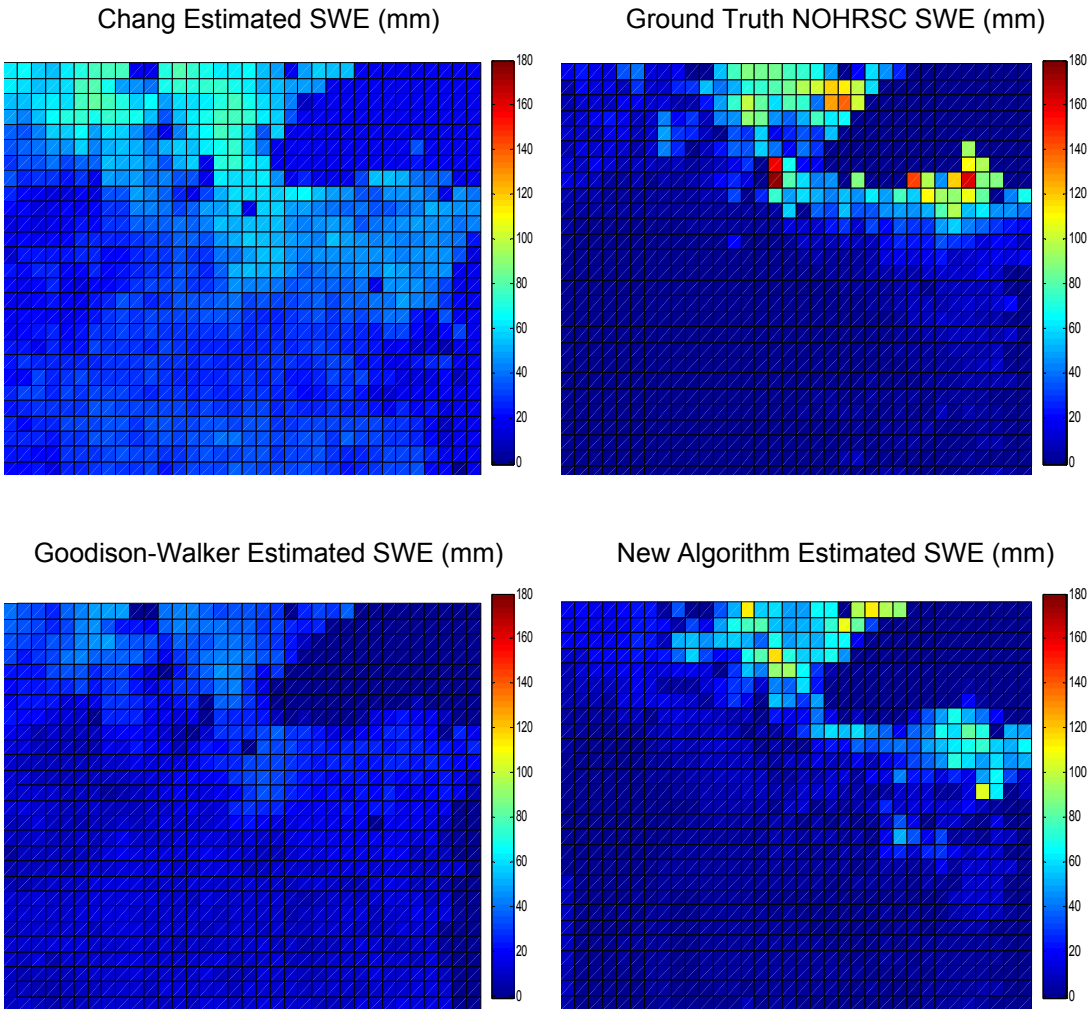

Figure 8. Comparison of estimated SWE by various algorithms with ground truth data for January 25, 2004 for the study area (Lat: 41N to 49N & Lon: -87W to-98W)

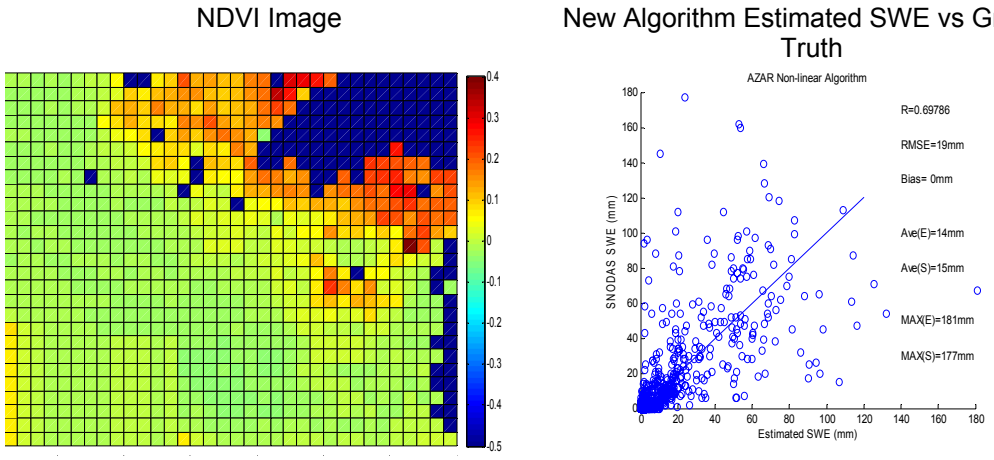

Figure 9. NDVI image and results of estimated SWE vs. ground truth for January 25, 2004 (left), Estimeted SWE by developed slgorithm vs. ground truth (right)

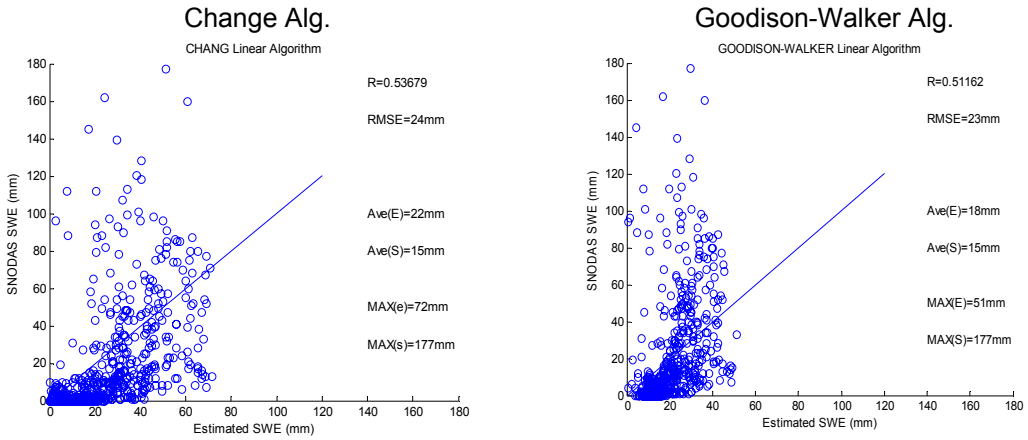

Figure 10. Results of estimated SWE using Chang and Goodison-Walker algorithm vs ground truth for January 25, 2004

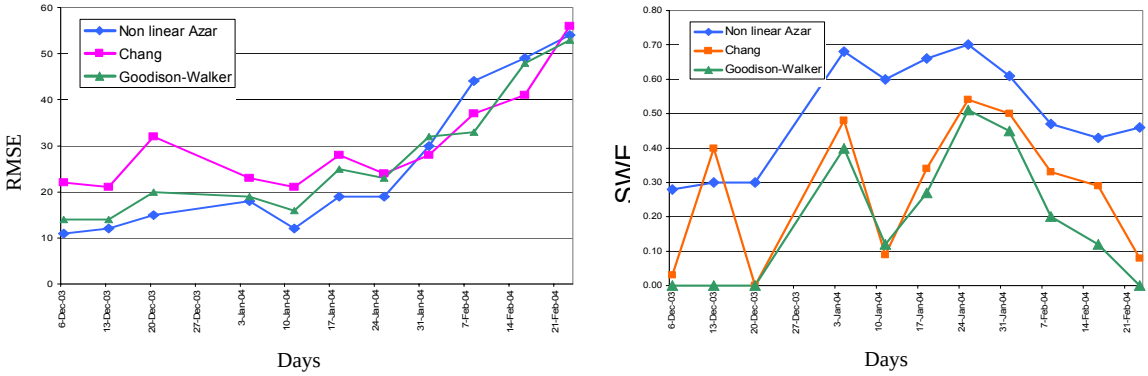

Figure 11. Variations of RMSE and Correlation Coefficients for selected days in winter 2003-2004

CONCLUSIONS

A non-linear method was developed to estimate SWE using SSM/I scattering Signatures and NDVI over Great Lakes area of the United States. Current linear algorithms such as Goodison-Walker and Chang algorithms are not sufficient for accurate estimations of SWE in Great Lakes area. In order to resolve this problem three winter seasons were studied. SSM/I data with corresponding snow depth, and snow water equivalent (SWE) were used to examine the sensors response to the changes in snow pack properties. SSM/I response in GTVN (19V-37V), GTH (19H-37H), and SSI (22V-85V) to snow depth or water equivalent changes were analyzed. In low latitudes, more southerly areas, with shallow snow SSI has the highest correlation with SWE. In higher latitudes GTVN and GTH are better estimators of SWE. However the slope of the relationship between the spectral signature and SWE varies with location. This variation of the slope was found to be correlated to NDVI and was used to develop the new algorithm to estimate SWE using SSM/I and NDVI. Validation of the new algorithm shows that it reduces the error of SWE estimates by more than 20 percent as compared to earlier linear algorithms such as Goodison-Walker or Chang algorithms. The analysis of derived SWE distributions over the study area also reveals a consistent improvement of retrieval accuracy of SWE by the new algorithm.

ACKNOWLEDMENTS

The authors express their gratitude to Dr C. Derksen of Meteorological Service of Canada (MSC) and Dr A. Frei of the City University of New York. The SNODAS datasets produced by NOHRSC, were obtained through NSIDC. Thanks to Dr T. Carrol at NOHRSC and L. Ballagh at NOAA at NSIDC, University of Colorado.

REFRENCES

Chang A.T.C., J. L. F., and D.K.Hall. (1987). "Nimbus-7 SMMR derived global snow cover parameters." Annals Glaciology 9: 39-44.

Derksen, R. B., A. Walker (2004). "Merging Conventional (1915-92) and Passive Microwave (1978-2002) Estimates of Snow Extent and Water Equivalent over Central North America." Journal of Hydrometeorology 5: 850-861.

Derksen C., A. W., B.Goodison (2005). "Evaluation of passive microwave snow water equivalent retrievals across the boreal forest/tundra transition of western Canada." Remote Sensing of Environment 96: 315-327.

De Seve D., B. M., Fortin J. P. , and Walker A., (1997). "Preliminary analysis of snow microwave radiometry using the SSM/I passive- microwave data: the case of La Grande River watershed (Quebec)." Annals of Geology 25.

Gates, David M. (1980) Biophysical Ecology, Springer-Verlag, New York, 611 p.

Grody N., B. N. (1996). "Global Identification of Snowcover Using SSM/I Measurements." IEEE Transaction on Geosciences and Remote sensing 34(1).

Hallikainen, M. T. (1984). "Retrieval of snow water equivalent from Nimbus-7 SSMR data: effect of land cover categories and weather conditions." IEEE Oceanic Eng 9(5): 372-376.

Kelly R.E., A. T. C., L.Tsang, J.L.Foster (2003). "A prototype AMSR-E Global Snow Area and Snow depth Algorithm." IEEE Transaction on Geosciences and Remote Sensing, 41(2): 230-242.

Kelly R.E.J. , A. T. C. C., J.L. Foster and D.K. Hall (2001). Development of a passive microwave global snow monitoring algorithm for the Advanced Microwave Scanning Radiometer-EOS.

Kurvonen, L. (1994). Radiometer measurements of snow in Sodankyla, Helsinki University of Technology, Laboratory of Space Technology.

Pullianen, J. T., Grandell J., and Hallikainen M (1999). "HUT snow emission model and its applicability to snow water equivalent retrieval." IEEE Transaction on Geosciences and Remote sensing 37(3): 1378-1390.

Rouse, J. W., R. H. Haas, J. A. Schell, and D. W. Deering (1973) 'Monitoring vegetation systems in the Great Plains with ERTS', Third ERTS Symposium, NASA SP-351 I, 309-317.

Tedesco M., P. J., Takala M., Hallikainen M., and Pampaloni P (2004). "Artificial neural network-based techniques for the retrieval of SWE and snow depth from SSM/I data." Remote sensing of Environment 90.

Walker, G. B. E. a. A. E. (1995). Canadian development and use of snow cover information from passive microwave satellite data. Passive microwave remote sensing of land- atmosphere interactions. B. J. Choudhury, Y. H. Kerr, E. G. Njoku and P. Pampaloni. The Netherlands, VSP BV 245-262.